nature communications

Article

https://doi.org/10.1038/s41467-025-57482-6

Structural basis for the allosteric activation of Lon by the heat shock protein LarA

Received: 18 November 2024

Accepted: 25 February 2025

Published online: 05 March 2025

Check for updates

Hsiu-Jung Wang[1], Yun-Erh Kuan[1], Meng-Ru Ho[1] ✉ & Chung-I Chang[1,2] ✉

Lon is a conserved AAA+ (ATPases associated with diverse cellular activities) proteolytic machine that plays a key regulatory role in cells under proteotoxic stress. Lon-mediated proteolysis can be stimulated by either the unfolded or specific protein substrates accumulated under stress conditions. However, the molecular basis for this substrate-controlled proteolysis remains unclear. Here, we have found that the heat shock protein LarA, a recently discovered Lon substrate and allosteric activator, binds to the N-terminal domain (NTD) of Lon. The crystal structure of the LarA-NTD complex shows that LarA binds to a highly conserved groove in the NTD through the terminal aromatic residue of its C-terminal degron. Crystallographic and biochemical evidence further reveals that this binding exposes the hydrophobic core of LarA, which can bind a leucine residue and promote local protein unfolding. These results define the mechanistic role of the NTD in regulating Lon-mediated proteolysis in response to varying cellular conditions.

To survive under various environmental conditions, such as heat shock that induces proteotoxic stress, cells depend on intracellular proteases to restore protein homeostasis (proteostasis) by removing damaged or misfolded proteins, or adjusting the levels of specific regulatory proteins[1]. In bacteria, Lon is the major protease responsible for maintaining cellular proteostasis under stressful conditions[2–4].

Lon belongs to the superfamily of AAA+ (ATPases associated with a variety of cellular activities) proteins and is ubiquitous in all kingdoms of life. Lon selects protein substrates by recognizing degradation tags, or degrons, which are specific sequences exposed in the terminal region of the protein substrates. It has been shown that Lon recognizes unfolded protein substrates containing degrons rich in hydrophobic or aromatic residues[5]. Interestingly, unfolded proteins or degron tags can allosterically stimulate Lon activity[3,6]. Moreover, several bacterial heat shock proteins, including LarA and HspQ, are also discovered as Lon substrates that function as the allosteric activators of Lon-mediated proteolysis via their C-terminal degrons[4,7]. In spite of these findings, the molecular mechanism of substrate- or degron-dependent activation of Lon has remained elusive.

Lon exerts its proteolytic function as a homohexamer. The polypeptide chain of Lon is folded into several domains or regions, which include an N-terminal domain (NTD), a long-helix region (LH), a AAA+ ATPase domain, and a protease domain (Fig. 1a). Cryo-EM structures of Lon have shown that the ATPase and protease domains form a hexameric complex with six AAA+ domains engaging a substrate polypeptide in a right-handed spiral staircase conformation and six proteolytic active sites located inside a hollow chamber[8–15]. Protruding from the AAA+ ring are six LHs, which form a triangular structure with three overlapping LHs to position six NTDs surrounding a central tri-tyrosine pore for substrate entry[10,11,14,16] (Fig. 1b). The six NTDs are flexible in the cryo-EM maps; but three of them with connecting LHs that do not interact mutually, are even more rotationally flexible (Fig. 1b). The NTD has long been suggested to mediate substrate recognition and the structures of isolated domains have been determined previously[17–19]. However, the NTD has no substrate-bound structure available and thus its mechanistic role in the function of Lon has remained elusive.

In this study, we have characterized the interaction of *Caulobacter crescentus* Lon (CcLon) with LarA, and found that LarA binds exclusively to the NTD of CcLon. Our structural and functional results show that the NTD and NTD-bound LarA form distinctive hydrophobic pockets that exhibit contrasting degron binding modes. Specifically, the former is non-permissive, while the latter complex is permissive, with regard to facilitating substrate unfolding and translocation driven

[1]Institute of Biological Chemistry, Academia Sinica, Taipei 11529, Taiwan. [2]Institute of Biochemical Sciences, College of Life Science, National Taiwan University, Taipei 10617, Taiwan. ✉e-mail: mho1@gate.sinica.edu.tw; chungi@gate.sinica.edu.tw

https://doi.org/10.1038/s41467-025-57482-6

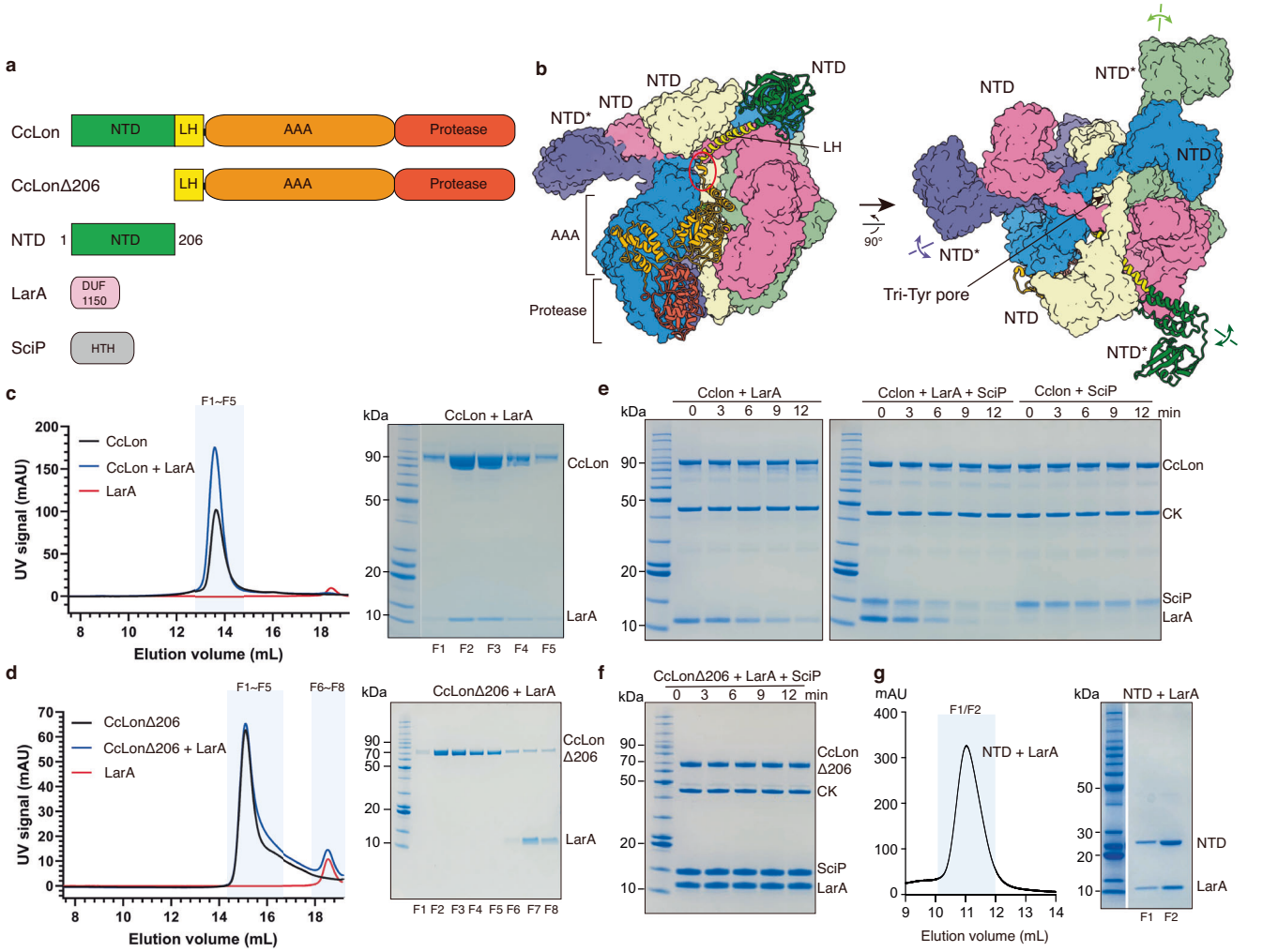

Fig. 1 | LarA binds specifically to the NTD of *C. crescentus* Lon. a Cartoon illustrating the composition of the protein constructs. NTD (green), LH (yellow), AAA (orange), and Protease (red) represent the N-terminal domain, long helices, ATPases Associated with diverse cellular Activities (AAA +) domain, and protease domain of CcLon, respectively. DUF (pink) is a domain of unknown function. HTH (grey) is helix-turn-helix. **b** Surface representations in side (left) and top (right) views of a hexameric Lon in a substrate-free state (PDB code 7YUX). Each protomer is colored differently. One protomer is shown in ribbons. Due to the linker between the LH and AAA domains (red oval), three of the NTDs (NTD*) are rotationally flexible. **c, d** Chromatograms of Superose 6 size-exclusion chromatography of full-length CcLon (**c**) and CcLonΔ206 (**d**), with or without the presence of LarA. The curves of CcLon/CcLonΔ206, LarA, and protein mixtures are labeled with black, red, and blue, respectively. **e** Degradation of LarA and SciP by CcLon. An ATP regeneration system using ATP, creatine phosphate, and creatine kinase (CK) was included in the reactions. **f** No ATP-dependent degradation of LarA or SciP by CcLonΔ206. **g** Chromatogram of Superdex 75 size-exclusion chromatography of purified LarA-NTD complex. SDS-PAGE and Coomassie staining were used to analyze selected chromatographic fractions and the in vitro reactions. The gels and curves (**c**–**g**) shown are representative of three independent experiments with consistent results. Source data are provided as a Source Data file.

by the AAA+ motor component of Lon. These results provide the mechanistic basis for understanding the allosteric activation of Lon-mediated proteolysis by LarA or other substrates.

Results

LarA binds to the NTD of CcLon

The heat shock protein LarA was previously identified from the cell lysates of *C. crescentus* by using a mass spectrometry (MS)-assisted trapping approach and its interaction with CcLon was detected by nativeMS[4]. We verified the binding of LarA to CcLon by using recombinant proteins, expressed and purified in *Escherichia coli*, and size-exclusion chromatography to analyze a mixture containing the two proteins (Fig. 1c). SDS-PAGE analysis of the eluted fractions containing full-length CcLon showed co-eluted LarA. However, when a mixture of LarA and CcLon-Δ206, a truncated CcLon variant lacking the NTD (aa. 1-206), was subject to a similar analysis, LarA did not co-eluted with the variant (Fig. 1d). These results suggest that LarA binds specifically to the NTD.

To investigate the allosteric activity of NTD, we examined the CcLon-mediated degradation of LarA or SciP, a helix-turn-helix (HTH) transcription factor essential for *Caulobacter* cell cycle regulation[20], and tested the effects of LarA on the degradation activity of CcLon and CcLon-Δ206 against SciP in vitro. Using SDS-Page gel assays, we found that LarA is efficiently degraded by CcLon, while SciP is degraded slowly (Fig. 1e). However, in the presence of LarA, both LarA and SciP are rapidly degraded by CcLon, consistent with the previous results[4]. By contrast, no degradation of LarA and SciP was observed by CcLon-Δ206, suggesting that NTD is essential to mediate the function of LarA (Fig. 1f).

To identify the LarA-NTD complex, we expressed His-tagged LarA and recombinant NTD without an affinity tag in *E. coli*, and we were able to purify the LarA-NTD complex from mixed cell lysates using Ni-nitrilotriacetic acid (NTA) and size-exclusion columns (Fig. 1g). Based on the location of the co-eluted peak from the latter, we concluded that LarA and NTD form a 1:1 heterodimer in solution.

https://doi.org/10.1038/s41467-025-57482-6

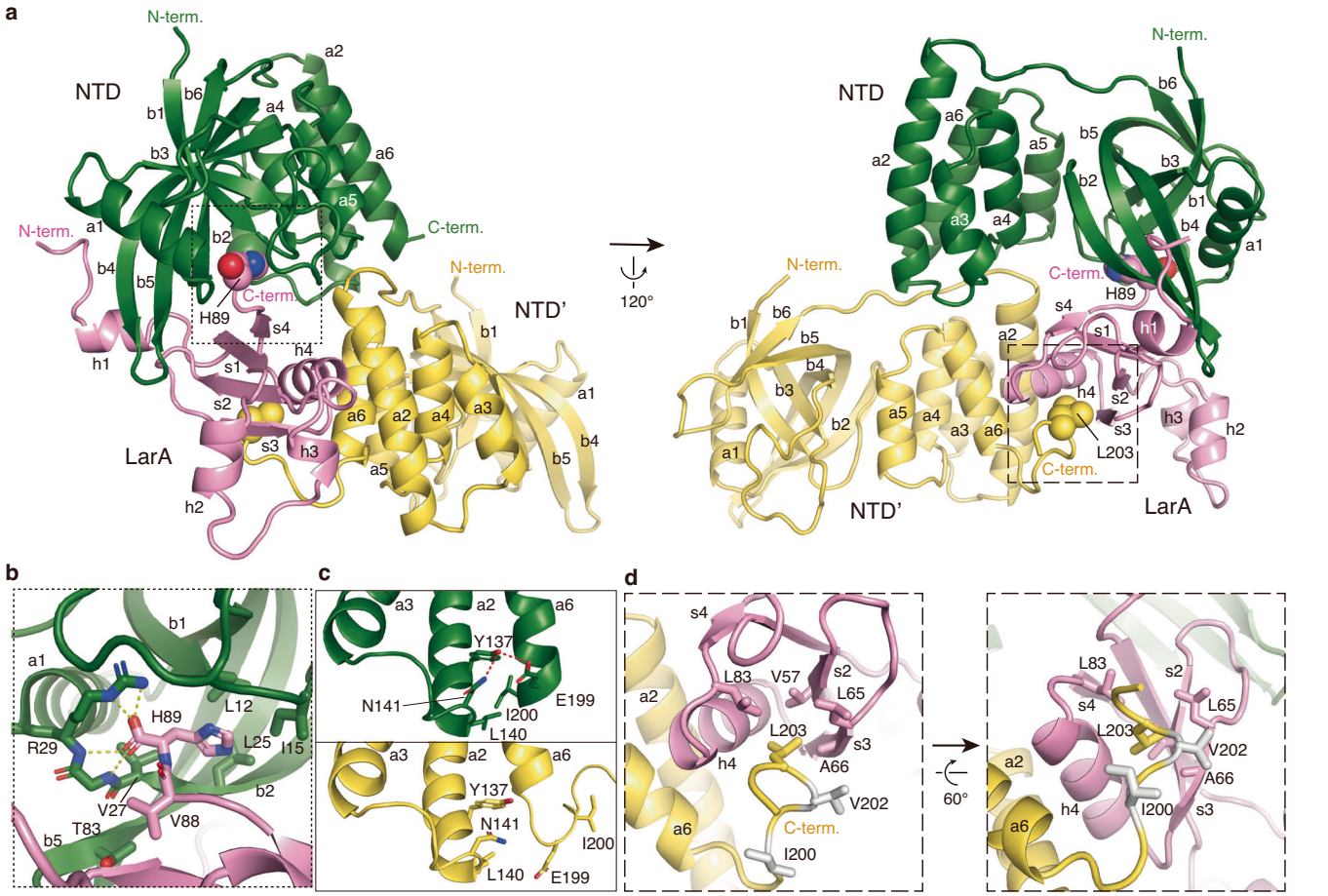

Fig. 2 | Structure of LarA bound to the NTD. a Ribbon diagrams of a complex consisting of one LarA (pink) bound to two NTD molecules (NTD: green and NTD′: gold) in the asymmetric unit (ASU) of the crystal. For clarity, the second LarA bound to NTD′ in the ASU is not shown. The amino-acid residue-binding sites identified in NTD and LarA were marked by a dotted box and a dashed box, respectively. **b** Close-up view of NTD bound to the C-terminal residue (His89) of LarA. The C-terminal and side-chain residues are shown in sticks. **c** Close-up view of the C-terminal helix of NTD and NTD′ showing the local unfolding of the latter, induced by LarA interaction (red dashed line). **d** Two close-up views of LarA bound to a leucine residue in the C-terminal tail of NTD′. Side chains of Val202 and Ile200 on NTD′ are labeled in grey for clear presentation.

The overall structure of LarA bound to the NTD

The LarA-NTD complex was crystallized in the tetragonal space group $P4_3$ with two heterodimers per asymmetric unit (ASU). The structure was determined at the resolution of 2.29 Å by molecular replacement, using search models of *C. crescentus* LarA and CcLon-NTD generated by AlphaFold[21]. Data collection and refinement statistics are given in Supplementary Table 1. CcLon-NTD contains two subdomains joined by a ten-residue linker (Fig. 2a). The N-terminal subdomain consists of one α-helix (a1) and six curved β-strands (b1-6), forming a fused double-barrel-like structure; the C-terminal subdomain forms a five-α-helix bundle (a2-6). LarA contains three short α-helices (h1-3) and a central core consists of a four-stranded β-sheet (s1-4) packed against an α-helix (h4) (Fig. 2a).

In the structure, the C-terminal aromatic residue (His89) of LarA binds to loop b2-a1, connecting strand b2 and helix a1, in the N-subdomain of NTD (Fig. 2b and Supplementary Fig. 1a, b). The carboxylic group of His89 forms polar interactions with the guanidinium group of Arg29 from the loop and the aromatic side chain binds to a hydrophobic pocket, formed by Leu25 of strand b2, as well as Leu12 and Ile15 of loop b1-b2 (Fig. 2b). Additionally, the penultimate residue Val88 of LarA makes hydrophobic contact at the interface with Thr83 from strand b5. However, it appears that only the binding of the C-terminal aromatic residue of LarA to the NTD pocket is specific, as the two NTD-bound LarA molecules in the ASU show significant rigid-body rotations (Supplementary Fig. 2).

Interestingly, we observed two different conformations of the C-terminal region of the two NTD molecules trapped in the crystal (chains b and d). This region is formed by residues 185-201, which corresponds to the N-terminal portion of the LH in full-length Lon. While this NTD region in chain d forms a long helix a6, the same region adopts a short helix with an unfolded C-terminal tail in chain b (Fig. 2c). This region in chains b and d is not involved in crystal contacts with any symmetry-related molecules. Unexpectedly, we found that an NTD-bound LarA molecule (chain c) binds to the C-terminal tail (aa. 197-205) of the NTD molecule (chain b) from the other heterodimeric complex in the asymmetric unit of the crystal. This coil region contains a cluster of three different hydrophobic residues (Ile200, Val202, and Leu203). Only Leu203 (Supplementary Fig. 1), but not the other two residues, binds to a conserved hydrophobic pocket of LarA composed of Val57, Leu65, and Leu83, which is formed by strands s2, s3, and helix h4 (Fig. 2d and Supplementary Fig. 3). Taken together, these structural results reveal a binding pocket of NTD for a C-terminal hydrophobic or aromatic residue and a binding pocket of LarA for a leucine residue. Importantly, local protein unfolding may be induced by interaction with LarA.

Amino-acid residue-binding pockets in the NTD and LarA

We conducted the mutational analysis to verify the functional significance of the conserved amino-acid residue-binding pockets identified in the NTD and LarA. We generated full-length CcLon mutants,

https://doi.org/10.1038/s41467-025-57482-6

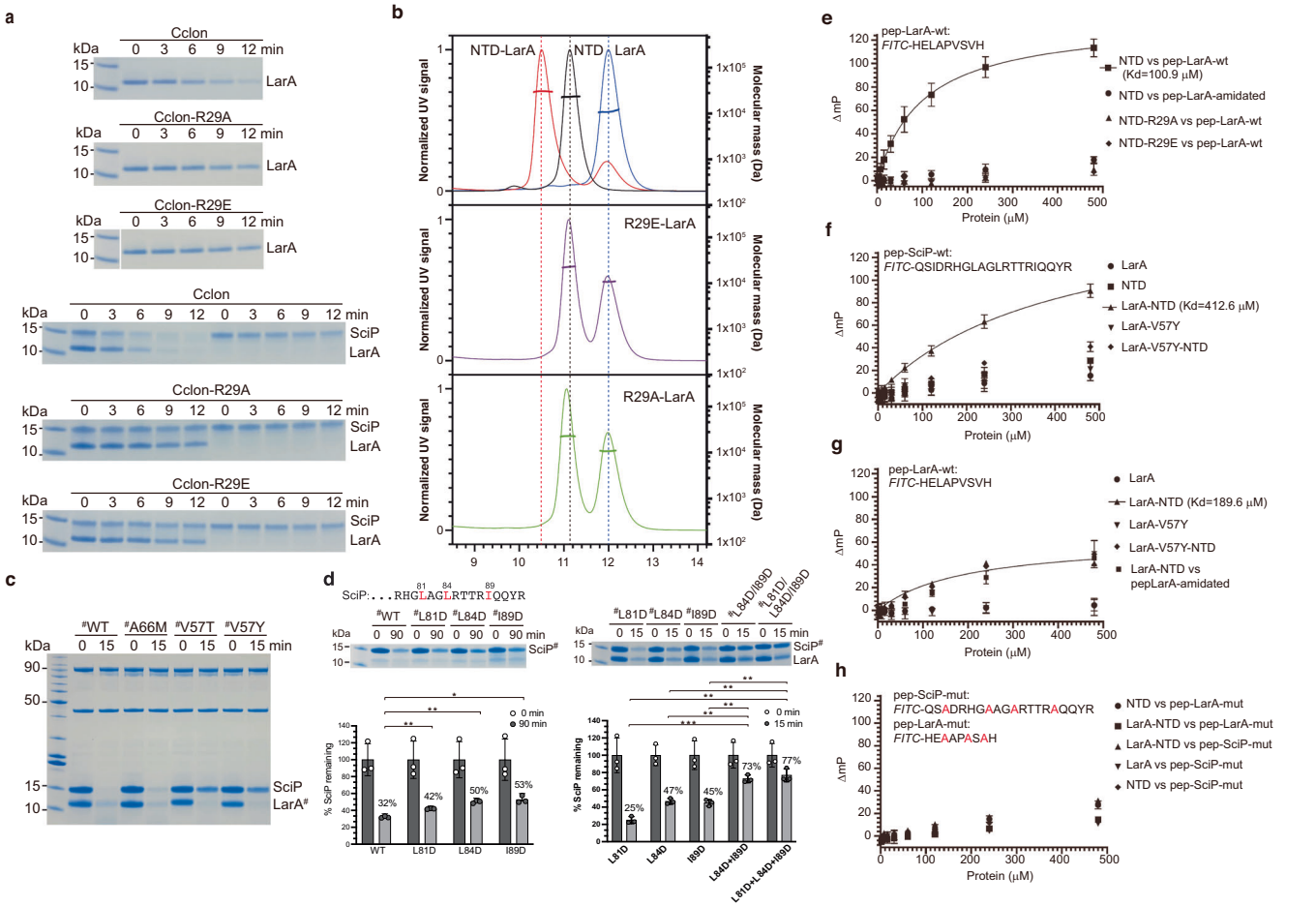

Fig. 3 | Mutational analyses of the amino-acid residue-binding pockets of the NTD and LarA. a In vitro reactions showing the essential role of Arg29 in the NTD of CcLon for LarA-mediated degradation of SciP. **b** SEC-MALS analysis showing the key role of Arg29 of the NTD in mediating LarA binding. **c**, In vitro reactions of CcLon demonstrating the important role of Val57 in the hydrophobic binding pocket of LarA for mediating SciP degradation. The gels shown in (**a**) and (**c**) are representative of three independent experiments with consistent results. Source data are provided as a Source Data file. **d** In vitro reactions investigating the role of the hydrophobic residues in the C-terminal degron of SciP for LarA-mediated degradation. Densitometry analysis of SciP remaining was performed for gel data run in triplicate. *p* values were calculated using an unpaired two-sided Welch's *t*-test. In the absence of LarA (left graph): L81D ($p = 0.0012$ **), L84D ($p = 0.0002$ ***), and I89D ($p = 0.0106$ *). In the presence of LarA (right graph): L81D vs. L84D + I89D ($p = 0.0002$ ***), L81D vs. L81D + L84D + I89D ($p = 0.0015$ **), L84D vs. L84D + I89D ($p = 0.0017$ **), L84D vs. L81D + L84D + I89D ($p = 0.0098$ **), I89D vs. L84D + I89D ($p = 0.0012$ **), and I89D vs. L81D + L84D + I89D ($p = 0.0074$ **). The number sign (#) in (**c**) and (**d**) denotes the various LarA or SciP constructs, which are either wild-type (wt) or with indicated mutations, used in the reactions. **e** Fluorescence polarization (FP) assays to detect the binding between different NTD constructs and fluorescein isothiocyanate (FITC) labeled peptides (pep-) derived from the C-terminal degron of LarA. **f, g** FP assays to detect the interaction of FITC-labeled peptides, derived from the wild-type (wt) C-terminal sequences of SciP (pep-SciP-wt)(**f**) or LarA (pep-LarA-wt)(**g**), with indicated proteins or protein complexes. **h** FP assays showing poor protein binding of the LarA or SciP peptides with all hydrophobic residues replaced by alanine (-mut). Data in (**d-h**) are presented as mean values ± SD; $n = 3$ independent measurements. Source data are provided as a Source Data file.

CcLon-R29A and -R29E, to test their degradation activity using LarA and SciP as the substrates. As described above, Arg29 of NTD is involved in polar interactions with the terminal residue of LarA. We found that CcLon-R29A and -R29E showed poor activity to degrade LarA compared to wild-type (WT) CcLon, in addition to their low activity against SciP (Fig. 3a). Importantly, the LarA-stimulated degradation activity of SciP was no longer observed by these mutants. We also prepared NTD-R29A and -R29E and the interaction of these single-domain mutants with LarA was investigated by using size-exclusion chromatography coupled to multi-angle light scattering (SEC-MALS). The results showed that NTD-WT binds to LarA and forms a peak corresponding to the 1:1 complex; however, NTD-R29A and -R29E failed to form a complex with LarA (Fig. 3b). Together, these results confirm the important role of Arg29 in mediating interaction with LarA.

Although the pocket-lining residues of the NTD of CcLon are highly conserved in other bacteria, such as *E. coli* and *B. subtilis*, we noticed that human LonP1 and *M. avium* contain an Asp residue instead of Arg29 as the carboxyl binding site; and a valine residue on the pocket is replaced by a threonine in *M. taiwanensis* (Supplementary Figs. 4a–f). Using a synthetic fluorescein-labeled peptide derived from the C-terminal degron (residues 81-89) of LarA (pep-LarA), we performed fluorescence polarization (FP) assays and found that the NTDs of the Lon proteins from these bacteria bind to the LarA peptide in various degrees, ranging being comparable to that of CcLon to modest binding, whereas MtaLon-NTD showed no binding to pep-LarA (Supplementary Fig. 4g). These results suggest a residue-binding preference for each NTD due to structural variation.

We prepared the mutant LarA-V57Y, designed to block the leucine-residue binding pocket of LarA, and analyzed its effect on stimulating SciP degradation by CcLon. We found that LarA-V57Y did not stimulate SciP degradation (Fig. 3c). Similarly, LarA-V57T, introducing a hydroxyl group into the pocket, also failed to do so. To further verify these results, we generated LarA-A66M containing a mutation that did

https://doi.org/10.1038/s41467-025-57482-6

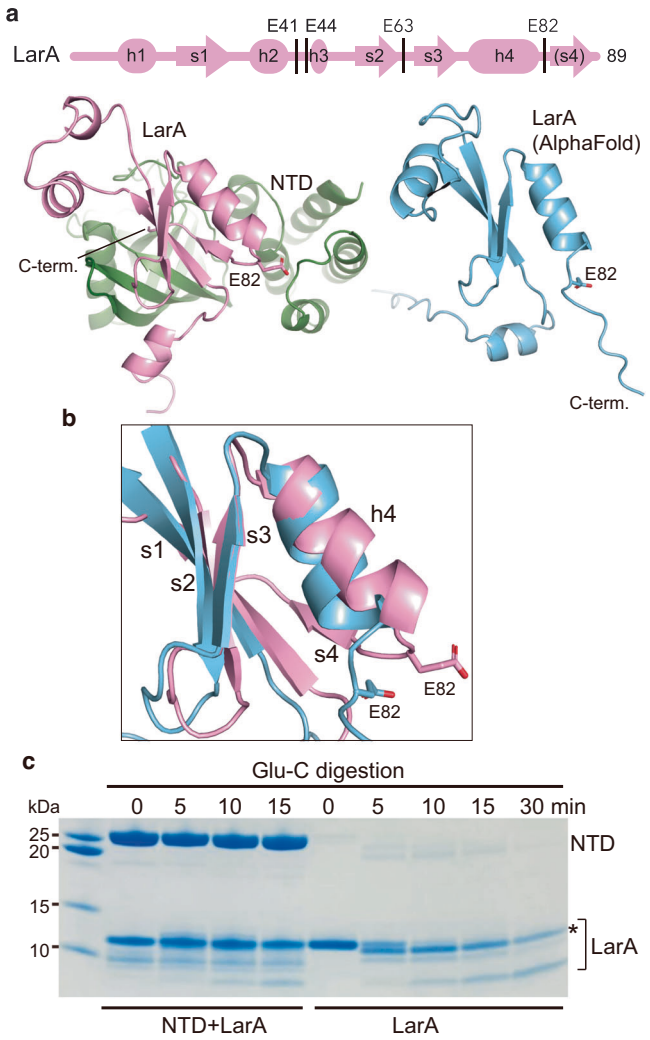

Fig. 4 | Conformational change of LarA induced by binding to the NTD. **a** Structure of the NTD-bound LarA (this work, pink) and that of free LarA (blue) predicted by AlphaFold, shown in ribbons in a similar orientation. An illustration of the secondary structure elements of the NTD-bound LarA is shown on top, with the Glu residues located in the loop regions marked. **b** Superimposition of the core structures of LarA in the NTD-bound and predicted free forms. **c** Limited proteolysis by the protease Glu-C of LarA in the presence and absence of the NTD. The LarA fragment corresponding to cleavage at the residue Glu82 is indicated by the asterisk. The gel shown is representative of two independent experiments with consistent results. Source data are provided as a Source Data file.

not impact the hydrophobic pocket of LarA based on the structure; as expected, this mutant showed normal stimulating activity. Therefore, we conclude that the leucine-residue binding pocket of LarA, as identified by crystallography, is functionally important for the LarA activity.

The C-terminal region of SciP contains three hydrophobic amino-acid residues (Leu81, Leu84, and Ile 89). If the hydrophobic-binding pocket of LarA is involved in binding to these residues, mutating these residues may impair SciP degradation. Therefore, we made single, double, or triple mutants of SciP accordingly. We found that the SciP mutants L84D and I89D were degraded less efficiently than the wild-type (WT) substrate. Moreover, SciP mutants with combined L84D and I89D mutations, or with all three residues mutated, were degraded even less efficiently by CcLon in the presence of LarA. (Fig. 3d). Collectively, these results demonstrate the important role of the C-terminal hydrophobic residues, especially Leu84 and Ile89, of SciP for LarA-dependent degradation by CcLon.

Binding of the NTD exposes the hydrophobic core of LarA

To ascertain whether the effects of the mutations in the NTD or LarA on substrate degradation correlate with their degron binding activity, we performed FP experiments using a series of fluorescein-labeled peptides derived from the C-terminal degrons of LarA and SciP to examine binding with NTD, LarA, or the LarA-NTD complex, with or without mutations of the binding pockets.

By the FP assays, we found that the NTD bound to pep-LarA, while NTD-R29A or -R29E did not (Fig. 3e), consistent with the degradation assay results. Additionally, no binding was observed of the NTD to a peptide with C-terminal amidation (Fig. 3e). These results suggest that R29 of the NTD forms a salt bridge with the C–terminus of LarA, which is important for binding interaction. Interestingly, neither the NTD nor LarA alone binds well to a fluorescent SciP peptide (pep-SciP), which contains a charged C-terminal residue (Fig. 3f). By contrast, a robust binding was observed for the LarA-NTD complex, but this activity was lost in the LarA-V57Y-NTD complex (Fig. 3f). When similar assays were performed using pep-LarA, no binding was observed with free LarA; however, both the LarA-NTD and LarA-V57Y-NTD complexes exhibited binding to pep-LarA (Fig. 3g). Importantly, we also found that the binding of LarA-NTD to pep-LarA-amidated is comparable to that of pep-LarA (Fig. 3g), which differs from the binding property of the NTD alone (Fig. 3e). Binding of the fluorescent peptides to the LarA-NTD complex was further confirmed by size-exclusion chromatography (Supplementary Fig. 5). Finally, we found that pep-SciP-mut or pep-LarA-mut, which lack hydrophobic residues in the sequences, failed to bind to NTD or the LarA-NTD complex (Fig. 3h).

Our FP results showing peptide binding of the LarA-NTD complex but not LarA alone suggests that a conformational change of LarA occurs upon binding to the NTD to expose a leucine-binding pocket. To validate these findings, we compared the structure of apo LarA predicted by AlphaFold with the crystal structure of the LarA-NTD complex. As shown in Fig. 4, the hydrophobic core of LarA is exposed only in the complex with the NTD to form the leucine-binding pocket, which is driven by the conformational change of the flexible C-terminal region of LarA to form strand s4 upon interaction with the NTD (Fig. 4a,b). To further confirm the AlphaFold model, we performed limited proteolysis by using the endoproteinase Glu-C, which is predicted to cleave LarA at the Glu82 if its C-terminal region is flexible. Indeed, we found that a corresponding truncated form of LarA is produced by incubation with Glu-C, which failed to do so when the NTD was mixed with LarA (Fig. 4c).

Discussion

In this crystallographic study, we report that the NTD of Lon binds to the C-terminal hydrophobic or aromatic residue of its substrate via a conserved pocket in the N-subdomain. We further show that LarA, a physiological substrate of Lon, exposes its hydrophobic core to form a leucine-binding pocket upon binding to the NTD through its C-terminal degron. The hydrophobic pockets of the NTD and NTD-bound LarA show distinct binding properties; the former binds specifically to the C-terminal aromatic or hydrophobic residues while the latter binds these residues that are internally located. The structure of LarA bound to the NTD shows a similar domain organization to cereblon (CRBN), a component of an E3 ubiquitin ligase complex, which is composed of an NTD-like N-terminal domain and a C-terminal thalidomide-binding domain (TBD)(Supplementary Fig. 6). However, the interaction of LarA with the NTD shows no similarity with that of TBD with the NTD-like domain in CRBN.

Using the FP assay, we determined a Kd value of 412.6 μM for the binding of the FITC-labeled SciP peptide to the LarA-NTD complex (Fig. 3f). The very weak binding observed suggests that additional stabilizing interactions, likely occurring between the full-length SciP

https://doi.org/10.1038/s41467-025-57482-6

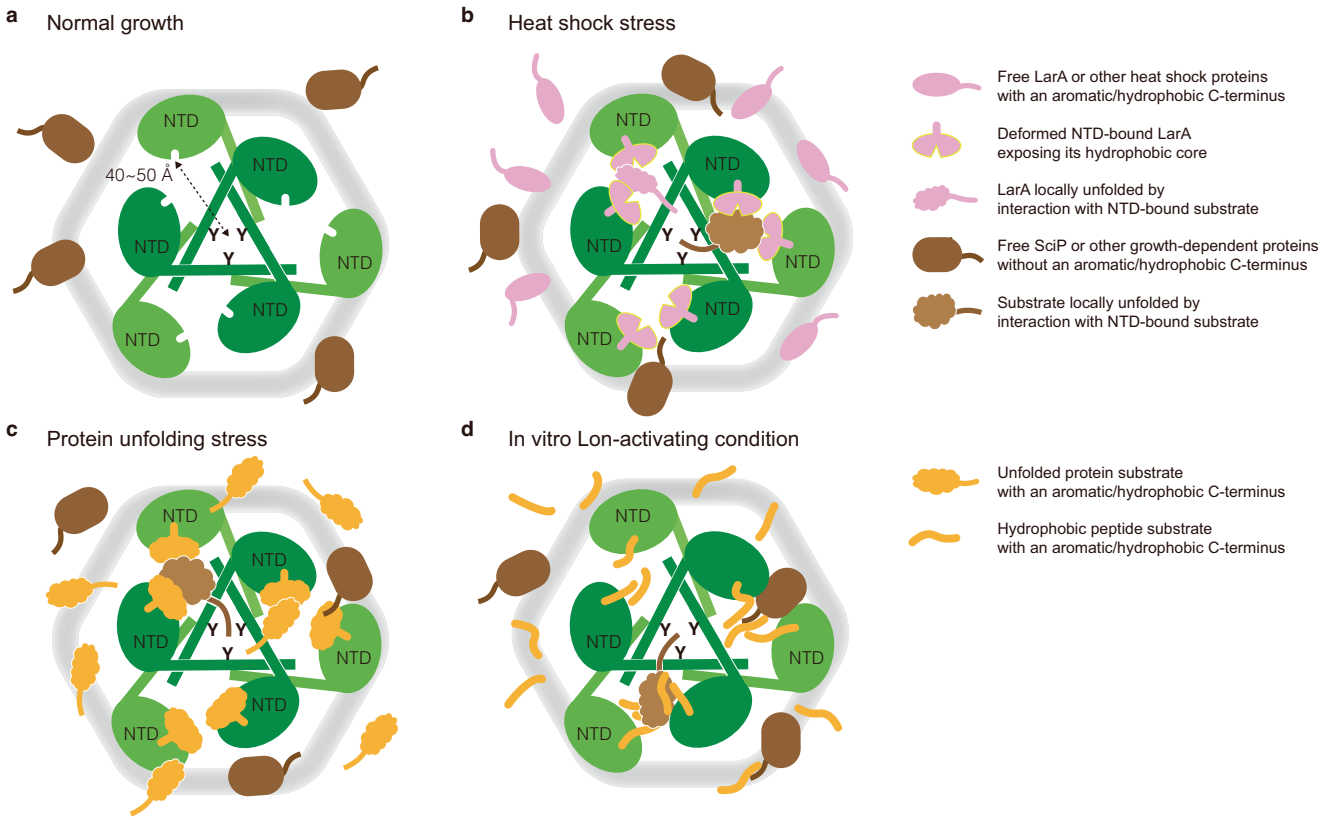

Fig. 5 | Model for the mechanistic role of the NTD in Lon-mediated proteolysis in bacteria under various environmental conditions. a Cartoon illustrating six NTDs distributed around the tri-tyrosine substrate-entry pore (denoted by three Ys) of hexameric Lon, drawn in top view. Each NTD harbors a binding pocket for the C-terminal aromatic or hydrophobic residues of the protein or peptide substrates. **b** An NTD can bind to a folded substrate, which is often overexpressed in cells under stress conditions, and induce a deformation to expose its hydrophobic core to mediate hydrophobic interactions with other substrate molecules of the same or different species, which leads to local or partially unfolding of protein substrates to facilitate binding of their C-terminal degrons to the triple tyrosine residues in the entry pore. Similar substrate-mediated hydrophobic interactions may occur by docking to the NTDs of unfolded protein substrates, which are accumulated in cells during protein unfolding stress (**c**) or degron peptides introduced to activate Lon-mediated proteolysis in vitro (**d**).

protein and multiple LarA-NTD modules within the context of full-length Lon, may enhance the overall affinity. However, attempts to measure the binding affinity of the full-length SciP using similar assays were unsuccessful due to its low labeling efficiency with a fluorescent dye.

Our crystal structure also provides evidence of protein unfolding effect mediated by NTD-bound LarA (Fig. 2c, d). The leucine-binding pocket of NTD-bound LarA in turn recognizes the hydrophobic residues in the C-terminal degron of SciP, which leads to the stimulation of SciP degradation by Lon. Based on these results, we propose a working model for the substrate- or degron-stimulated substrate degradation by Lon, in which the NTD plays a crucial role in regulating Lon-mediated proteolysis in response to various physiological stress or in vitro conditions. In this tentative model, a folded substrate, such as LarA, binds to the NTD through a C-terminal aromatic or hydrophobic residue. The NTD-bound substrate adopts a deformed conformation to expose a hydrophobic pocket, allowing it to interact with the aromatic or hydrophobic residues in the C-terminal region of other substrate molecules, whether from the same or different species (Fig. 5a, b). Alternatively, the exposed pocket may interact with an adjacent NTD, triggering conformational changes that reveal distinct binding sites for the substrates. According to the depicted model, a damaged or misfolded substrate, or a degron peptide, which are expected to carry exposed hydrophobic patches, may bind similarly to the NTD via the C-terminal residue and act as the receptors for hydrophobic or aromatic residues (Fig. 5c, d). Furthermore, we envision that docking of these substrates or degron peptides to the six NTDs of Lon provides and distributes multiple hydrophobic surfaces around the tri-tyrosine entry pore; these hydrophobic patches act not only directly as the degron receptors, they may also serve as catalyst for the unfolding of the interacting substrate, which has been frequently observed in hydrophobic interaction chromatography and by molecular simulations[22–24]. The dual-process of substrate-mediated binding and unfolding allows for cooperative binding of the same substrate species[6], as well as combinatorial interaction between different substrates, such as LarA and SciP. We presume that this NTD-mediated dual-process may facilitate binding of the substrates' C-terminal tails to the central tri-tyrosine pore and granting their access to the AAA-protease machinery assembly of Lon for processive translocation and degradation reactions.

To date, two other regulatory proteins have been reported to activate Lon-mediated proteolysis. The heat shock protein HspQ, found in many Gram-negative bacteria, exhibits LarA-like properties by enhancing Lon-mediated degradation of various substrates[7,25,26]. Additionally, the adaptor protein SmiA in *Bacillus subtilis* mediates Lon-dependent degradation of SwrA through hybrid priming and scaffolding mechanisms[27–29]. We propose that HspQ likely stimulates Lon-dependent proteolysis via a LarA-like mechanism involving its binding to the NTD. In contrast, SmiA appears to function differently, as it does not interact directly with Lon but instead binds with high affinity to its client, SwrA[29]. However, we hypothesize that SmiA's priming effect, which converts SwrA from a protease-resistant to a protease-sensitive state, may involve a LarA-like conformational change induced by the NTD. Structural analyses of the interactions

between HspQ, SmiA, Lon proteins, and their client substrates will be critical for elucidating their molecular mechanisms.

Finally, we demonstrate the functional conservation of NTDs in other Lon proteins by showing that the NTDs of various Lon proteins can bind to a degron peptide of LarA (Supplementary Fig. 4g). Notably, the NTD of *E. coli* Lon exhibits strong binding to the LarA peptide, despite the absence of LarA in *E. coli*. These findings suggest the possible existence of yet-to-be-identified LarA-like proteins in *E. coli* or even in eukaryotic cells, which may modulate Lon activity by interacting with the NTD.

Methods

Cloning and mutagenesis

The full-length *C. crescentus* Lon (CcLon) was cloned into the bacterial expression vector pET21a(+) with a C-terminal 6×His tag (GenScript). Quick-change mutagenesis was performed based on this plasmid to make the N-terminal domain of CcLon (NTD; aa. 1-206) without a His-tag by adding a stop codon after Lysine 206. Additionally, the NTD fragment was cloned into pET28a(+) with a C-terminal 6×His tag. LarA was cloned into pET21a(+) with a N-terminal 6×His tag (GenScript). SciP was cloned into pET28a(+) with a N-terminal 6×His tag followed by a T7 tag. Single mutants of NTD (R29A and R29E), LarA (A66M, V57Y, and V57T), and SciP (L81D, L84D, I89D) were performed by site-directed mutagenesis, as well as the double mutant (L84D/I89D) and triple mutant (L81D/L84D/I89D) of SciP. CcLon with the NTD removed (CcLonΔNTD) was cloned into pET21a(+) (GenScript). All constructs in this study were verified by the DNA Sequencing Core Facility of Academia Sinica. Sequences of the primers are listed in Supplementary Table 2.

Protein expression and purification

Plasmid-transformed BL21(DE3) cells were plated onto agar plates containing LB/carbenicillin (50 μg/mL) or kanamycin (25 μg/mL), and incubated overnight at 37 °C. A single colony was picked and cultured in 3 ml LB for 2 hr at 37 °C. The culture was transferred to 20 ml LB and incubated for 2 hr at 37 °C. 10 ml of the culture was added into 1 liter LB medium containing antibiotics, and incubated at 37 °C and 250 rpm until the OD_{600} reached 0.6 to 0.8. Isopropyl β-d-thiogalactopyranoside (IPTG) was added to the cell culture at 1 mM working concentration, and the cell culture was incubated overnight at 20 °C and 150 rpm. Cells were harvested by centrifugation at 6000 rpm (JLA-8.1000 rotor, Beckman) for 20 minutes at 4 °C and cell pellets were suspended in the lysis buffer (50 mM Tris-HCl pH 8.0 and 250 mM NaCl, 5% glycerol). The cell lysate was first ruptured by a French press (Avestin) at 15,000–20,000 psi and centrifuged at 30,000 x g (JA-25.50 rotor, Beckman) for 30 min at 4 °C. The supernatant was incubated with Ni-nitrilotriacetic acid (Ni-NTA) resins (Qiagen) at 4 °C for 2 h. The resins were subsequently washed with 15 mM imidazole and then eluted with 250 mM imidazole. The Ni-NTA eluted proteins were further applied to a HitrapQ column for NTD and LarA, or a HitrapS column for SciP. The eluted proteins were subjected to size-exclusion chromatography (SEC) on a Superdex 75 (Cytiva), the columns pre-equilibrated with 20 mM Tris-HCl (pH 8.0), 200 mM NaCl, and 1 mM DTT. For CcLon and CcLon-Δ206, the Ni-NTA eluted proteins were subjected to size-exclusion chromatography on a Superose 6 Increase (Cytiva), the columns pre-equilibrated with 20 mM Tris-HCl (pH 8.0), 200 mM NaCl, 10 mM $MgCl_2$ and 1 mM DTT. The eluted fractions from size-exclusion chromatography were examined by SDS-PAGE and used for FP binding and Lon activity assays.

Crystallization and data collection

To prepare the LarA-NTD complex for crystallization, cells in equal amounts expressing untagged NTD and His-tagged LarA were mixed; the proteins were extracted and purified by ion exchange and size-exclusion chromatography as mentioned above. Fractions containing the complex were pooled and concentrated to 22 mg/mL. Crystals were grown at 22 °C by hanging-drop vapor diffusion method, by mixing 1 μl of protein solution with 1 μl of well solution containing 20% PEG 20000, 0.1 M sodium citrate, pH 5.0, and 3% w/v D-(+)-glucose monohydrate. Before data collection, the crystals were cryoprotected in reservoir solution supplemented with 20% PEG 400. Complete X-ray diffraction data sets to 2.69 and 2.29 Å resolutions were collected respectively on beamlines 07 A at Taiwan Photon Source (TPS) and BL-1A at Photon Factory (KEK, Japan).

Structure determination

Phasing was initially performed on the 2.69 Å data set by molecular replacement, using the search models consisting of the coordinates of the NTD and LarA of *C. crescentus* predicted by AlphaFold 2[21], successfully yielded an electron-density map with sufficient quality. The final structure was refined using the 2.29 Å data set by iterative cycles of manual refitting using Coot[30], model rebuilding by Autobuild in Phenix[31], and reciprocal-space refinement in Refmac5[32]. Crystallographic and refinement statistics are listed in Supplementary Table 1.

Fluorescence polarization (FP)

NTD, LarA, the LarA-NTD complex, and NTD mutant proteins were serially diluted from 480 μM to 1.875 μM and mixed with FITC-labeled peptides, with concentrations adjusted based on solubility and fluorescence intensity. FP was measured in triplicate using a Spark multimode microplate reader (TECAN, Switzerland) at 485 nm (excitation) and 535 nm (emission). The FP values were expressed in millipolarization (mP) and calculated using the following equation:

$$mP = 1000 \times (I^{Par} - G \times I^{Per})/(I^{Par} + G \times I^{Per})$$

where I^{Par} is the parallel emission intensity, I^{Per} is the perpendicular emission intensity, and G is the grating factor, set to 1.059 by the Spark reader. Changes in polarization (ΔmP) were calculated by subtracting the control value, and plotted against protein concentrations in a scatter plot. Data were analyzed and fitted to calculate binding constants (Kd) using GraphPad Prism 10.3.1 (GraphPad Software, LLC).

Size-exclusion chromatography coupled to multi-angle light scattering (SEC-MALS)

SEC – MALS measurements were performed using a miniDAWN TREOS detector (Wyatt Technology Corporation) coupled to an Agilent 1260 Infinity HPLC. Samples of NTD, LarA, and 1:1 molar ratio mixtures of LarA-NTD, LarA-NTD-R29A, and LarA-NTD-R29E were prepared at a concentration of 30 μM for SEC analysis. A 100 μL aliquot of each sample was injected into an ENrich SEC 70 size exclusion chromatography column (Bio-Rad), pre-equilibrated with running buffer (25 mM HEPES, pH 7.5, 200 mM NaCl, 1 mM DTT). The chromatography was carried out at a constant flow rate of 0.5 mL/min, with UV absorbance monitored at 280 nm. Molecular weights were determined by multi-angle laser light scattering using an in-line miniDAWN TREOS detector and an Optilab T-rEX differential refractive index detector (Wyatt Technology Corporation). Bovine serum albumin (Sigma, A1900) was used to calibrate the system. Data were analyzed using ASTRA 6 software (Wyatt Technology Corporation), using a dn/dc value of 0.185 mL/g, and plotted with GraphPad Prism 10.3.1 (GraphPad Software, LLC).

Substrate degradation assay

CcLon-WT (0.125 μM, calculated as hexamer) was incubated in the reaction buffer containing 20 mM Tris-HCl (pH 8.0), 200 mM NaCl, and 10 mM $MgCl_2$, 1 mM DTT, plus 4 mM ATP, 75 ug/ml creatine kinase (CK) at 30 °C for 2 min, then 4 μM SciP or 6 μM LarA or both were added to the reaction mixture (total 300 μL) and incubated at 30 °C. Reactions were stopped at different times by adding 16.7 μL 5× gel-loading dye in a 50 μL reaction mixture and heating at 95 °C

for 10 min. To compare Cclon activity on SciP WT and its mutants, with or without LarA WT or its mutants, 10 μM of each substrate was used. Substrate degradation was assessed by SDS-PAGE and Coomassie Blue staining, and quantified using integrated density measurement in ImageJ 1.54 g.

Statistical analysis

Kinetics analysis was conducted using saturation test (specific binding, one site) in GraphPad Prism 10.4.1, and statistical significance was assessed using *t*-tests. *P*-values were calculated to evaluate the statistical significance of the estimated differences.

Reporting summary

Further information on research design is available in the Nature Portfolio Reporting Summary linked to this article.

Data availability

The structural factors and coordinates have been deposited in the Protein Data Bank under the accession code 9JWA. Source data are provided with this paper.

References

1. Balchin, D., Hayer-Hartl, M. & Hartl, F. U. In vivo aspects of protein folding and quality control. *Science* **353**, aac4354 (2016).
2. Tsilibaris, V., Maenhaut-Michel, G. & Van Melderen, L. Biological roles of the Lon ATP-dependent protease. *Res. Microbiol.* **157**, 701–713 (2006).
3. Jonas, K., Liu, J., Chien, P. & Laub, M. T. Proteotoxic stress induces a cell-cycle arrest by stimulating Lon to degrade the replication initiator DnaA. *Cell* **154**, 623–636 (2013).
4. Omnus, D. J. et al. The heat shock protein LarA activates the Lon protease in response to proteotoxic stress. *Nat. Commun.* **14**, 7636 (2023).
5. Gur, E. & Sauer, R. T. Recognition of misfolded proteins by Lon, a AAA(+) protease. *Genes Dev.* **22**, 2267–2277 (2008).
6. Gur, E. & Sauer, R. T. Degrons in protein substrates program the speed and operating efficiency of the AAA+ Lon proteolytic machine. *Proc. Natl. Acad. Sci. USA* **106**, 18503–18508 (2009).
7. Puri, N. & Karzai, A. W. HspQ functions as a unique specificity-enhancing factor for the AAA+ Lon protease. *Mol. Cell* **66**, 672–683.e4 (2017).
8. Shin, M. et al. Structures of the human LONP1 protease reveal regulatory steps involved in protease activation. *Nat. Commun.* **12**, 3239 (2021).
9. Shin, M. et al. Structural basis for distinct operational modes and protease activation in AAA+ protease Lon. *Sci. Adv.* **6**, eaba8404 (2020).
10. Coscia, F. & Löwe, J. Cryo-EM structure of the full-length Lon protease from *Thermus thermophilus*. *FEBS Lett.* **595**, 2691–2700 (2021).
11. Li, S. et al. Complete three-dimensional structures of the Lon protease translocating a protein substrate. *Sci. Adv.* **7**, eabj7835 (2021).
12. Li, S. et al. Molecular basis for ATPase-powered substrate translocation by the Lon AAA+ protease. *J. Biol. Chem.* **297**, 101239 (2021).
13. Li, S. et al. Processive cleavage of substrate at individual proteolytic active sites of the Lon protease complex. *Sci. Adv.* **7**, eabj9537 (2021).
14. Mohammed, I. et al. Catalytic cycling of human mitochondrial Lon protease. *Structure* **30**, 1254–1268.e7 (2022).
15. Yang, J., Song, A. S., Wiseman, R. L. & Lander, G. C. Cryo-EM structure of hexameric yeast Lon protease (PIM1) highlights the importance of conserved structural elements. *J. Biol. Chem.* **298**, 101694 (2022).
16. Li, S. et al. A 5+1 assemble-to-activate mechanism of the Lon proteolytic machine. *Nat. Commun.* **14**, 7340 (2023).
17. Tzeng, S.-R. et al. Molecular insights into substrate recognition and discrimination by the N-terminal domain of Lon AAA+ protease. *Elife* **10**, e64056 (2021).
18. Chen, X. et al. Crystal structure of the N domain of Lon protease from *Mycobacterium avium* complex. *Protein Sci.* **28**, 1720–1726 (2019).
19. Li, M. et al. Structure of the N-terminal fragment of *Escherichia coli* Lon protease. *Acta Crystallogr. D. Biol. Crystallogr.* **66**, 865–873 (2010).
20. Tan, M. H., Kozdon, J. B., Shen, X., Shapiro, L. & McAdams, H. H. An essential transcription factor, SciP, enhances robustness of *Caulobacter* cell cycle regulation. *Proc. Natl Acad. Sci. USA* **107**, 18985–18990 (2010).
21. Jumper, J. et al. Highly accurate protein structure prediction with AlphaFold. *Nature* **596**, 583–589 (2021).
22. Jungbauer, A., Machold, C. & Hahn, R. Hydrophobic interaction chromatography of proteins. III. Unfolding of proteins upon adsorption. *J. Chromatogr. A* **1079**, 221–228 (2005).
23. Patel, A. J. et al. Extended surfaces modulate hydrophobic interactions of neighboring solutes. *Proc. Natl Acad. Sci. Usa.* **108**, 17678–17683 (2011).
24. Yu, L., Zhang, L. & Sun, Y. Protein behavior at surfaces: orientation, conformational transitions and transport. *J. Chromatogr. A* **1382**, 118–134 (2015).
25. Shimuta, T.-R. et al. Novel heat shock protein HspQ stimulates the degradation of mutant DnaA protein in *Escherichia coli*. *Genes Cells* **9**, 1151–1166 (2004).
26. Yeom, J. & Groisman, E. A. Activator of one protease transforms into inhibitor of another in response to nutritional signals. *Genes Dev.* **33**, 1280–1292 (2019).
27. Mukherjee, S. et al. Adaptor-mediated Lon proteolysis restricts *Bacillus subtilis* hyperflagellation. *Proc. Natl. Acad. Sci. USA* **112**, 250–255 (2015).
28. Hughes, A. C., Subramanian, S., Dann, C. E., 3rd & Kearns, D. B. The C-terminal region of *Bacillus subtilis* SwrA is required for activity and adaptor-dependent LonA proteolysis. *J. Bacteriol.* **200**, (2018).
29. Olney, S. G., Chien, P. & Kearns, D. B. SmiA is a hybrid priming/scaffolding adaptor for the LonA protease in *Bacillus subtilis*. *J. Biol. Chem.* **298**, 102045 (2022).
30. Emsley, P. & Cowtan, K. Coot: model-building tools for molecular graphics. *Acta Crystallogr. D. Biol. Crystallogr.* **60**, 2126–2132 (2004).
31. Liebschner, D. et al. Macromolecular structure determination using X-rays, neutrons and electrons: recent developments in Phenix. *Acta Crystallogr D. Struct. Biol.* **75**, 861–877 (2019).
32. Murshudov, G. N. et al. REFMAC5 for the refinement of macromolecular crystal structures. *Acta Crystallogr. D. Biol. Crystallogr.* **67**, 355–367 (2011).

Acknowledgements

We thank the staff at the Photon Factory BL1A and Taiwan Photon Source 07 A beamlines for assistance with data collection. We acknowledge the technical expertise of the synthesis core facility in the Institute of Biological Chemistry at Academia Sinica for fluorescent peptide synthesis. This work was supported by Academia Sinica (AS-IA-112-L03 to C.I.C) and National Science and Technology Council of Taiwan (NSTC111-2320-B-001-013-MY3 to C.I.C).

Author contributions

Conceptualization: C.I.C.; methodology: H.J.W., Y.E.K., M.R.H., C.I.C.; investigation: H.J.W., Y.E.K., M.R.H., C.I.C.; Visualization: H.J.W., Y.E.K., M.R.H., C.I.C.; Funding acquisition: C.I.C.; Project administration: C.I.C.; Supervision: C.I.C.; Writing – original draft: H.J.W., M.R.H., C.I.C.; Writing – review & editing: H.J.W., M.R.H., C.I.C.

Competing interests

The authors declare no competing interests.

Additional information

Supplementary information The online version contains supplementary material available at https://doi.org/10.1038/s41467-025-57482-6.

Correspondence and requests for materials should be addressed to Meng-Ru Ho or Chung-I Chang.

Peer review information *Nature Communications* thanks the anonymous reviewer(s) for their contribution to the peer review of this work. A peer review file is available.